

Protocol
Physikal.-chem. Praktikum 165.008
K4 - Oxalic Acid Oxidation

Group F

Jonas Adamer (12225913)

Florian Fitsch (12218283)

Leonhard Ritt (12208881)

Date of experiment: 2024/10/21

Date of submission:

Contents

1	Objective	1
2	Experiment	1
2.1	Determination of Absorbance Maximum of KMnO_4	1
2.2	Creation of Calibration Curve for KMnO_4	1
2.3	Measurement of the Autocatalyzed Redox Reaction of KMnO_4 and Oxalic Acid	1
2.4	Measurement of the Mn^{2+} -Catalyzed Redox Reaction of KMnO_4 and Oxalic Acid . .	2
2.5	Measurement of the Acid-Base Reaction of Phenolphthalein and Sodium Hydroxide . .	2
3	Results and Discussion	3
3.1	Absorbance Maximum and Calibration Curve of KMnO_4	3
3.2	Determination of Reaction Order of Redox Reaction	5
3.3	Determination of Reaction Order of Acid-Base Reaction	7
4	Conclusion	7
A	Plots of Further Oxalic Acid Oxidation Experiments	8

1 Objective

In this assignment, the kinetics of chemical reactions are studied through two separate experiments.

In the first experiment, the redox reaction between oxalic acid and potassium permanganate is studied: After determining the absorbance maximum of potassium permanganate, a series of solutions is produced and measured as a calibration for concentration of permanganate as a function of absorbance. Finally, the change in permanganate-concentration is measured in-situ, both with and without a catalyst, in order to determine the reaction order.

In the second experiment, the acid-base reaction between phenolphthalein and sodium hydroxide is studied. The absorbance of the reaction mixture is also measured in-situ and the reaction order regarding phenolphthalein is determined.

2 Experiment

2.1 Determination of Absorbance Maximum of KMnO_4

In order to find the absorbance maximum, 79 mg of potassium permanganate were weighed out, dissolved in deionized water and diluted in a 50 mL volumetric flask, yielding a 0.01 mol/L solution. 5 mL of this solution were taken out and once again diluted in a 50 mL flask, yielding a concentration of 1 mmol/L.

2 mL of the prepared solution were filled into a cuvette and inserted into the photometer. Its absorbance was then measured in wavelength increments of 10 nm between 450 nm and 600 nm. For each wavelength, the photometer was calibrated by setting values of 0% and 100% transmission, using an opaque block and a cuvette filled with deionized water, respectively. Since high absorbances were measured at 530 nm and 550 nm, another series of measurements was taken between 520 nm and 560 nm with increments of 2 nm. Using this process, a maximum at 532 nm was determined.

2.2 Creation of Calibration Curve for KMnO_4

To create the calibration, the 1 mmol/L potassium permanganate solution, which was prepared in Section 2.1, was further diluted to prepare six further solutions, with concentrations of 0.75, 0.60, 0.50, 0.40, 0.25 and 0.10 mmol/L. After calibrating the photometer as described in Section 2.1, the absorbance values of the seven solutions were measured at the previously determined wavelength of 532 nm. To account for inaccuracies, each measurement was taken three times, with the cuvette being filled with fresh solution after every measurement.

2.3 Measurement of the Autocatalyzed Redox Reaction of KMnO_4 and Oxalic Acid

By further diluting the 10 mmol/L solution prepared in 2.1, a solution with a concentration of 4 mmol/L was prepared. Additionally, a 40 mmol/L solution of oxalic acid was obtained by dissolving 0.505 g oxalic acid dihydrate in deionized water using a 100 mL volumetric flask. Additionally, a sulfuric acid solution of about 24 w% was prepared by combining three parts water with one part concentrated (96 %) sulfuric acid.

To start the reaction, 10 mL of the oxalic acid solution, 0.4 mL of the sulfuric acid and 4 mL of the potassium permanganate solution were added to a beaker and mixed thoroughly. A stopwatch was started once the permanganate solution was added. After filling 2 mL of the mixture into a cuvette, absorbance measurements were taken every 10 seconds, until the measured value reached 0 or stopped changing. This experiment was repeated two more times.

2.4 Measurement of the Mn^{2+} -Catalyzed Redox Reaction of KMnO_4 and Oxalic Acid

By dissolving 0.340 g manganese sulfate in deionized water in a 50 mL volumetric flask, a 40 mmol/L solution was prepared.

Three reactions were measured as described in Section 2.3, with the addition of adding 0.2 mL of the prepared manganese sulfate solution to the reaction mixture before measuring it.

2.5 Measurement of the Acid-Base Reaction of Phenolphthalein and Sodium Hydroxide

By diluting 7.5 mL of 2 mol/L sodium hydroxide with deionized water in a 50 mL volumetric flask, 50 mL of a 0.3 mol/L solution was prepared. Additionally, by dissolving 877 mg of sodium chloride in deionized water and diluting to 50 mL, a 0.3 mol/L solution was prepared.

By diluting the former with the latter solution, small amounts of solutions with sodium hydroxide concentrations of 0.2, 0.1 and 0.05 mol/L, were prepared.

2 mL of each of the four solutions were then transferred into a cuvette, and a drop of phenolphthalein was added. The cuvettes were inserted into the photometer, which was set at 532 nm¹, and, after dropping to an absorbance value of 0.8, further measurements were taken every 30 seconds over a span of six minutes. Since the time available for the experiment ran out, only one sample of each concentration was measured. The final sample (0.05 mol/L) did not reach the starting absorbance of 0.8 in time, and as such, higher absorbance values were recorded and used for the evaluation of this sample.

¹Due to an error, the desired wavelength of 550 nm was not set before starting the experiment

3 Results and Discussion

3.1 Absorbance Maximum and Calibration Curve of KMnO_4

The recorded absorbances of potassium permanganate are plotted as an absorbance spectrum in Figure 1. The determined absorbance maximum is at 532 nm. While literature records a maximum at 526 nm², the discrepancy to the found value may be due to a number of factors such as imprecise photometer calibration or differences in cuvette materials and/or cleanliness.

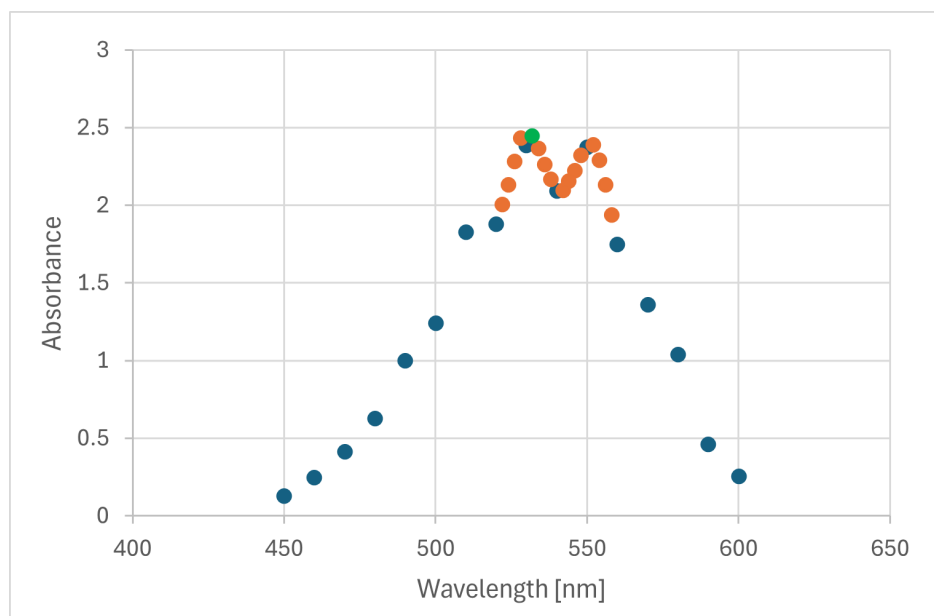


Figure 1: Absorbance spectrum of KMnO_4 at wavelengths between 450 and 600 nm. The blue dots show the measurements of the first scan, which was taken in 10 nm increments, while the orange dots mark the measurements of the second scan (2 nm increments). The absorbance maximum at 532 nm is shown in green.

²P Gomes, R Fernandes, and Wellington Lyra. “Flow-injection spectrometric determination of sodium diclofenac in pharmaceutical formulations”. In: *Journal of the Chilean Chemical Society* 63 (2018), pp. 3941–3946. doi: 10.4067/s0717-97072018000203941.

Figure 2 shows the calibration curve (created through linear regression) for the concentration of potassium permanganate as a function of absorbance. In order to ensure higher accuracy at very low concentrations, the curve was constrained to show an absorbance of zero at a concentration of 0 mol/L. As can be seen, linearity, and thus the validity of the Beer-Lambert law is given for the entire tested concentration range.

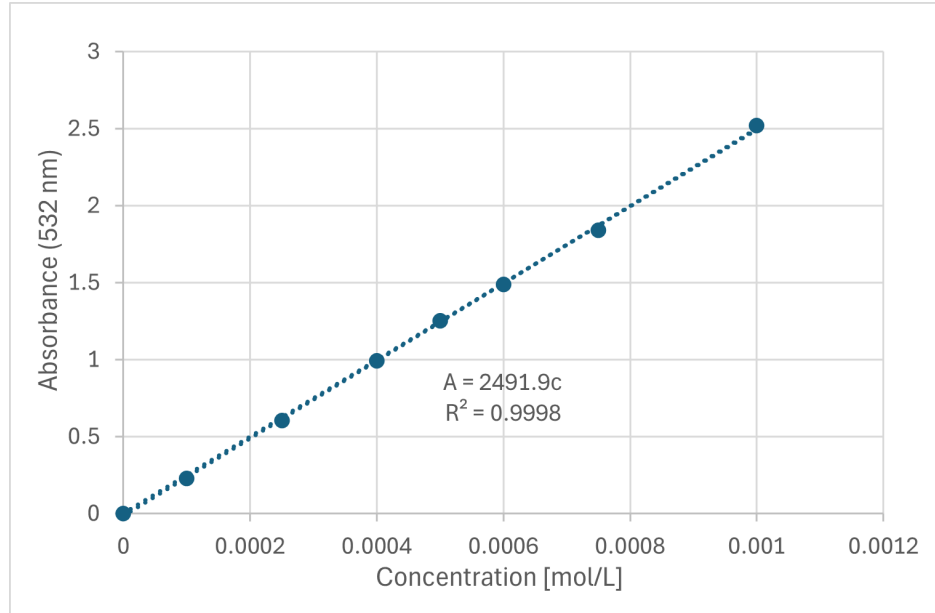


Figure 2: Average values of measured absorbance plotted against potassium permanganate concentration. A calibration curve is fit to the data using linear regression.

By inserting the resulting linear equation $A = 2491.9 \cdot c$ into the Beer-Lambert law (Equation 1), rearranging and inserting the known cuvette length of 1 cm, the molar attenuation coefficient ε can be calculated for a wavelength of 532 nm:

$$A = \varepsilon \cdot c \cdot d = 2491.9 \cdot c \quad (1)$$

$$\varepsilon = \frac{2491.9}{d} = 2491.9 \quad (2)$$

where: A = Absorbance

ε = Molar attenuation coefficient [$\text{L mol}^{-1} \text{cm}^{-1}$]

c = Concentration of sample [mol/L]

d = Path length through sample (cuvette length) [cm]

3.2 Determination of Reaction Order of Redox Reaction

By rearranging the Beer-Lambert law (Equation 1), the concentration of a sample can be determined from a given absorbance value.

$$c = \frac{A}{\varepsilon \cdot d} = \frac{A}{2491.9} \quad (3)$$

The resulting concentrations can then be plotted according to the rate laws of zeroth, first and second order, which are shown in Table 1.

Table 1: Rate equations and their integrated forms for reactions of zeroth, first and second order.

0th Order	1st Order	2nd Order
$-\frac{dc}{dt} = k$	$-\frac{dc}{dt} = k \cdot c$	$-\frac{dc}{dt} = k \cdot c^2$
$c = c_0 - k \cdot t$	$\ln c = \ln c_0 - k \cdot t$	$\frac{1}{c} = \frac{1}{c_0} + k \cdot t$

The following Figures 3 and 4 show the respective concentrations during the autocatalyzed and Mn^{2+} -catalyzed redox reactions of oxalic acid with potassium permanganate plotted against time according to the integrated rate equations shown above. For each plot, a curve has been fit using linear regression, with the coefficient of determination R^2 calculated as a means to assess linearity.

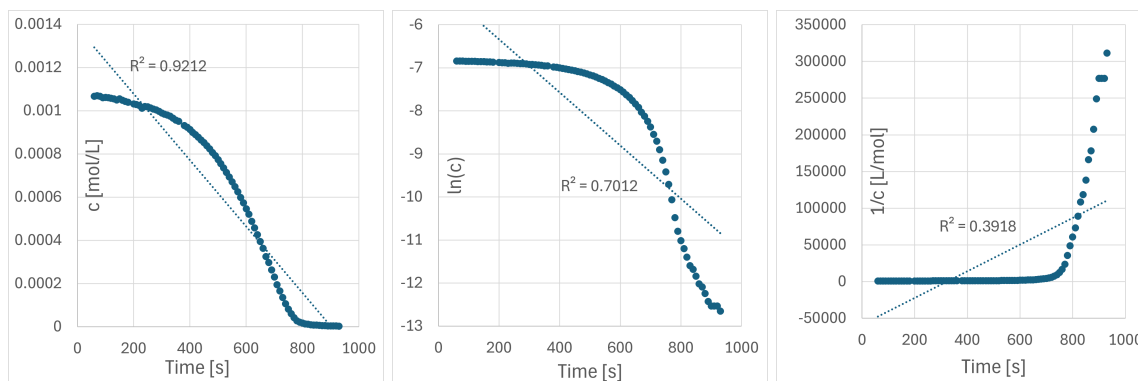


Figure 3: Measured concentrations during the first of three autocatalyzed redox reactions plotted against time according to the integrated rate equations of zeroth order (left), first order (center) and second order (right). Lines are fit to each plot using linear regression and the corresponding R^2 -values shown.

As can be seen from the displayed coefficients of determination of the autocatalyzed reaction, the highest linearity is observed at zeroth order. If one considers however, that a system undergoing autocatalysis will have a reduced reaction speed at the start, it follows that systems in which a reaction usually proceeds quickly at first before slowing down over time as reactand concentration sinks (as is the case in first and second order reactions), may have a worse fit. As such, it is uncertain from this data, whether the indication of a zeroth order reaction by the displayed linearity values is true to reality.

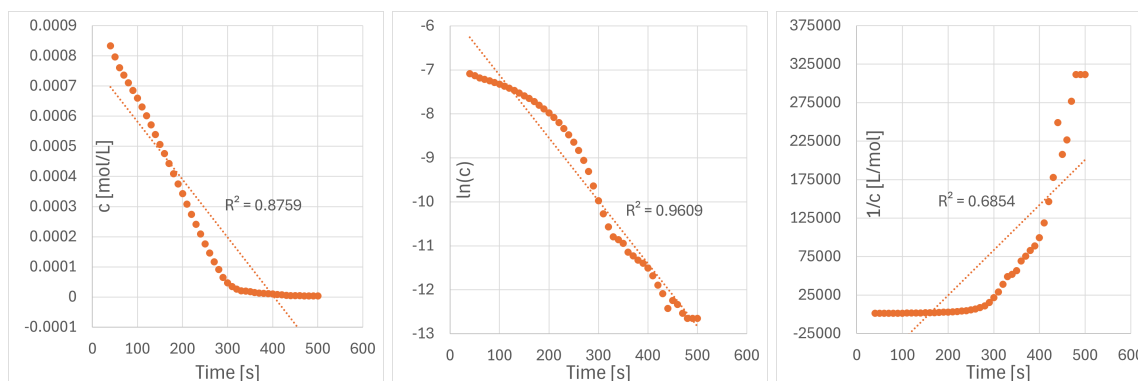


Figure 4: Measured concentrations during the first of three Mn^{2+} -catalyzed redox reactions plotted against time according to the integrated rate equations of zeroth order (left), first order (center) and second order (right). Lines are fit to each plot using linear regression and the corresponding R^2 -values shown.

Looking at the coefficients of determination of the Mn^{2+} -catalyzed reaction, the highest linearity is found for the first order rate equation. However, a high linearity is also observed for a zeroth order reaction, while the first order reaction visibly deviates from the regression line at the start of the experiment. This hump in the first order plot, as well as the lack of apparent concavity in part of the zeroth order plot (which would be expected if the system was of first order), might be explained by the production of additional Mn^{2+} -ions during the reaction, further catalyzing and thus speeding it up after an initial delay.

Comparing the two figures above - in particular the graphs of zeroth order - the differences between the studied types of catalysis become apparent: while the autocatalyzed reaction proceeds very slowly at first before speeding up as time proceeds and slowing down as the permanganate concentration approaches zero, the Mn^{2+} -catalyzed reaction shows a rather steady reaction speed, plummeting towards the end.

Thus, while the coefficients of determination gathered from the autocatalyzed reaction indicate a reaction of zeroth order, it is assumed - for reasons stated in the above paragraphs - that the first order reaction shown by studying the linearities of the plots of the Mn^{2+} -catalyzed reaction is more accurate to reality.

Additionally, this assumption more closely matches expectations from looking at the reaction from a theoretical standpoint: a second-order reaction might be expected due to the fact that two separate reactants are involved; however, due to the high excess of oxalic acid (10 times the stoichiometric amount), the system might more accurately follow first order kinetics, resulting in a pseudo first order reaction.

3.3 Determination of Reaction Order of Acid-Base Reaction

In order to determine the reaction order, the measured absorbance (which is proportional to the concentration of phenolphthalein) was plotted against time according to the integrated rate equations shown in Table 1.

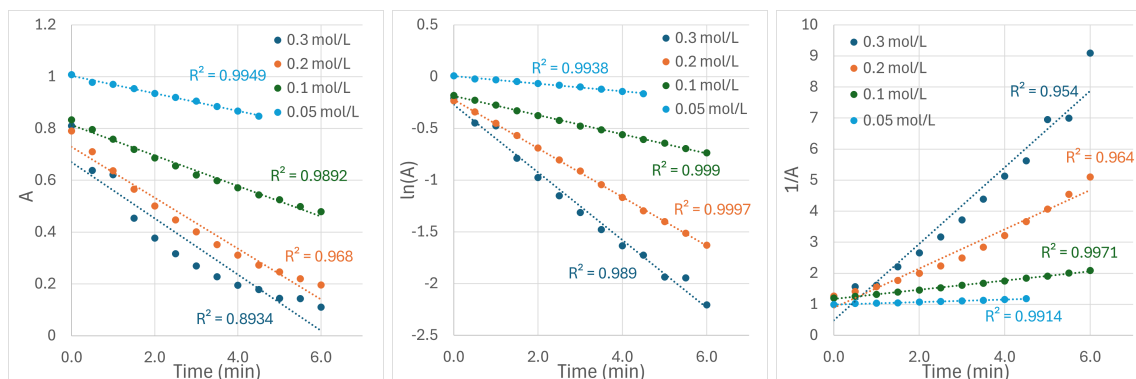


Figure 5: Measured absorbance values during the reactions of phenolphthalein with different concentrations of sodium hydroxide plotted against time according to the integrated rate equations of zeroth order (left), first order (center) and second order (right). Lines are fit to each plot using linear regression and the corresponding R^2 -values shown.

The linear regression curves shown in the figure above and their coefficients of determination show that, for every concentration other than 0.05 mol/L, a reaction of first order most closely fits the recorded data. This matches the theoretical expectation of a pseudo first order reaction, since the concentration of sodium hydroxide is several orders of magnitude greater than that of phenolphthalein and can thus be considered static over the course of the experiment. Nonetheless, it is apparent that, with higher sodium hydroxide-concentrations, the reaction proceeds at a higher rate, which further suggests that the reaction is not strictly first-order.

4 Conclusion

Through in-situ absorption measurements, the kinetics of an autocatalyzed and a regularly catalyzed redox-reaction, as well as an acid-base reaction were studied.

While the data recorded from the autocatalyzed redox reaction of potassium permanganate and oxalic acid indicated a zeroth order reaction, the data from the catalyzed reaction pointed towards first order kinetics. Ultimately, a first order reaction was deemed the more accurate model of reality when considering both experimental data as well as theoretical expectations.

The acid-base reaction of phenolphthalein and sodium hydroxide too, was determined to most closely follow the kinetics of a first order reaction, although a dependency of the reaction speed to the concentration of sodium hydroxide was observed, indicating a second order (pseudo first order) reaction instead.

Appendices

A Plots of Further Oxalic Acid Oxidation Experiments

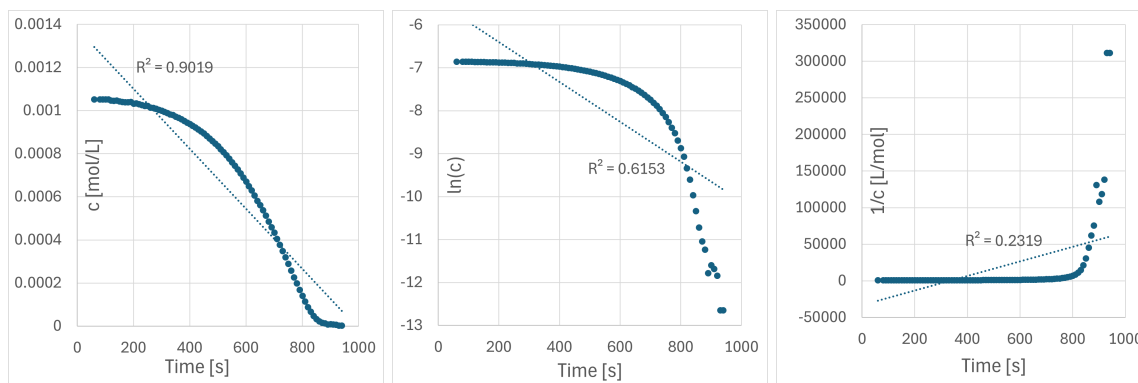


Figure 6: Measured concentrations during the second of three autocatalyzed redox reactions plotted against time according to the integrated rate equations of zeroth order (left), first order (center) and second order (right). Lines are fit to each plot using linear regression and the corresponding R^2 -values shown.

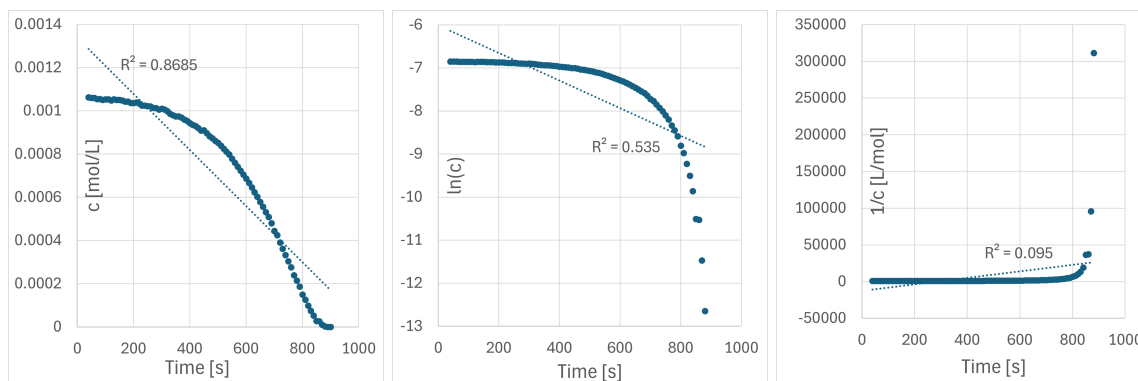


Figure 7: Measured concentrations during the third of three autocatalyzed redox reactions plotted against time according to the integrated rate equations of zeroth order (left), first order (center) and second order (right). Lines are fit to each plot using linear regression and the corresponding R^2 -values shown.

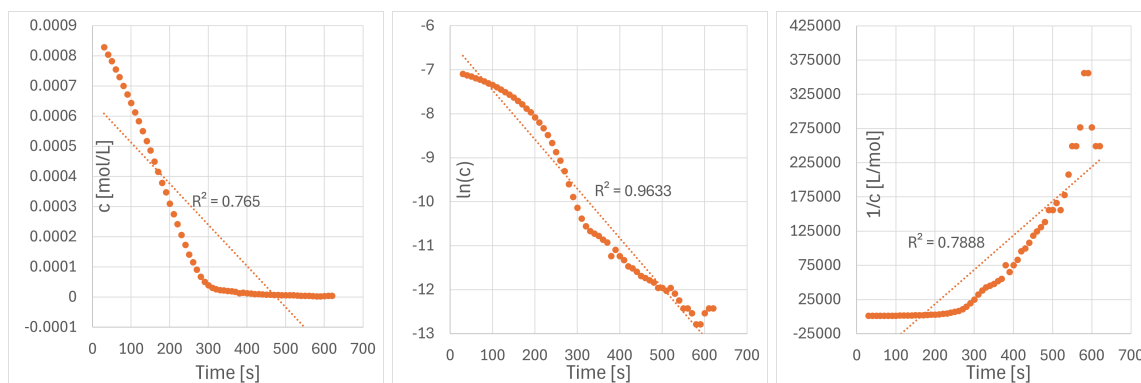


Figure 8: Measured concentrations during the second of three Mn^{2+} -catalyzed redox reactions plotted against time according to the integrated rate equations of zeroth order (left), first order (center) and second order (right). Lines are fit to each plot using linear regression and the corresponding R^2 -values shown.

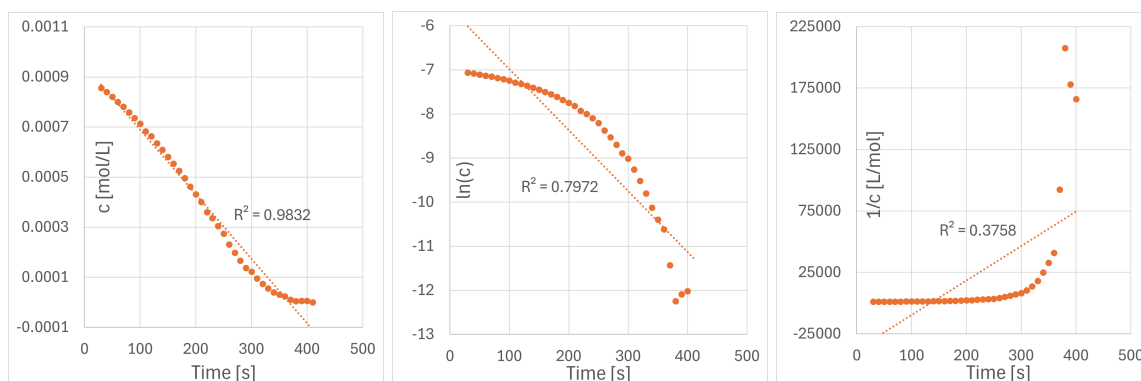


Figure 9: Measured concentrations during the third of three Mn^{2+} -catalyzed redox reactions plotted against time according to the integrated rate equations of zeroth order (left), first order (center) and second order (right). Lines are fit to each plot using linear regression and the corresponding R^2 -values shown.